Anti-prostate cancer activity and mechanism of the sesquiterpenoid lactone THA from Cyanthillium cinereum

Wenfeng Wang
Wuyi University
Man Xiao
Wuyi University
Peng Hong
Wuyi University
Danyu Huang
Macao University Science and Technology
Liting Liu
Wuyi University
Xi Zheng
Wuyi University
Song Ang
Wuyi University
Dongli Li
wyuchemldl@126.com
Wuyi University

Research Article

Keywords: Cyanthillium cinereum, Prostate cancer, Sesquiterpenoid lactone, Apoptosis, Xenograft tumor

Posted Date: February 24th, 2026

DOI: https://doi.org/10.21203/rs.3.rs-8798804/v1

Additional Declarations: No competing interests reported.

Anti-prostate cancer activity and mechanism of the sesquiterpenoid lactone THA from *Cyanthillium cinereum*

Wenfeng Wang [a], Man Xiao [a], Peng Hong [a], Danyu Huang [c], Liting Liu [a], Xi Zheng [a,b**], Song Ang [a,b], Dongli Li [a,b,*]

[a] *School of Pharmacy and Food Engineering, Wuyi University, Jiangmen, Guangdong Province, 529020, China*

[b] *International Healthcare Innovation Institute (Jiangmen), Jiangmen, Guangdong Province, 529040, China*

[c] *State Key Laboratory of Quality Research in Chinese Medicine, Macao University Science and Technology, Macao, 999078, China.*[1]

[*]Corresponding author.

E-*mail addresses*: wyuchemldl@126.com (D. Li).

[**]Corresponding author.

E-*mail addresses*: wyuchemxzh@126.com (X. Zheng).

Abstract

Purpose: This study aims to evaluate the *in vitro* effect of 8α-tigloyloxyhirsutinolide-13-O-acetate (THA) on human prostate cancer cells and to examine its *in vivo* inhibitory effect on tumor growth in a mouse xenograft model.

Methods: In this study, the androgen-independent prostate cancer (AIPC) cell line PC-3 was employed. To investigate the effects of THA, we assessed cell proliferation, migration, invasion, apoptosis, and cell cycle distribution using MTT, wound healing, Transwell invasion, colony formation assays, Hoechst-33342 staining and flow cytometry. A mouse xenograft tumor model was established, and treatment groups received THA. The expression levels of p-STAT3, p-AKT, p-Erk1/2, CDK2, cyclin E1, MMP9, Bcl-2, Bax, and survivin were analyzed by Western blotting. Tumor formation and progression were evaluated by monitoring tumor volume.

Results: Our study showed that THA strongly inhibited cell growth and induced apoptosis, as well as caused cell cycle arrest at the S phase in PC-3 cells. THA also strongly suppressed cell migration and invasion, and decreased spheroid and colony formation. Animal experiment showed that THA inhibited the growth of PC-3 xenograft tumor in nude mice. Studies on mechanisms of actions showed that the potent anti-prostate cancer effects of THA were associated with inhibition of STAT3, AKT, and Erk1/2 pathways.

Conclusion: Our findings demonstrate that the potent anti-prostate cancer activity of THA is associated with inhibition of the STAT3, AKT, and Erk1/2 pathways. These data lend support to the further investigation of THA as a potential therapeutic agent against prostate cancer.

Keywords: *Cyanthillium cinereum*, Prostate cancer, Sesquiterpenoid lactone, Apoptosis, Xenograft tumor.

1. Introduction

Prostate cancer is the most commonly diagnosed cancer and second leading cause of cancer-related death in men in Western countries (Siegel et al. 2024). Currently, the effective treatment for the androgen sensitive prostate cancer is hormone deprivation (McDonald et al. 2022) However, the prostate cancer cells lose their hormone dependence and therapeutic responsiveness during hormone deprivation treatment (McDonald et al. 2022; Desai et al. 2021), and the disease progresses to an androgen-independent stage with no effective therapeutic options at present (Gulley et al. 2003). Treatment of these patients with chemotherapy may prolong their lives, but toxicity and other side effects are serious problems of chemotherapy (Aparicio et al. 2013; Huebner et al. 2020). Therefore, novel treatment options including naturally occurred compounds with strong anticancer activity are of great significance for the management of prostate cancer patients.

Cyanthillium cinereum (L.) H. Rob. (Asteraceae) has many medicinal and civilian values, and their leaves and inflorescences are often used as traditional Chinese medicine or folk herbs to treat various diseases (Trang et al. 2024). The leaves and inflorescences of *C. cinereum* are rich in various bioactive components, such as volatile oils, flavonoids, triterpenoids, alkaloids, etc (Sulaiman et al. 2022; Chadwick et al. 2013). These ingredients endow *C. cinereum* with various pharmacological activities, including anti-inflammatory, antioxidant, antibacterial, antipyretic, cough suppressant, sedative, diuretic, and other effects. Therefore, in traditional medicine, *C. cinereum* are widely used to treat various diseases such as colds, coughs, fever and arthritis (Iwalewa et al. 2003; Neamsuvan et al. 2012; Lin 2005). Although the compounds with anti-tumor activity in this plant have attracted significant attention, but the current pharmacological activity research in this aspect still needs to be further explored. In a recent study, our laboratory has isolated a series of sesquiterpenoid compounds from *C. cinereum*, and 8α-tigloyloxyhirsutinolide-13-*O*-acetate (THA) was found to exert anti-prostate cancer activity (Ang et al. 2023). It is of great interest to further explore the anticancer activities and mechanisms of actions for this compound using suitable *in vitro* and *in vivo* models.

In the present study, the effects of THA on cell viability, apoptosis, migration and invasion were determined in cultured prostate cancer cells. The *in vivo* anti-prostate cancer effect THA was also determined using a mouse xenograft model. Our study showed that THA inhibited the proliferation and stimulated apoptosis in prostate cancer cells, and also strongly decreased cell migration and invasion. Moreover, THA inhibited the growth of prostate xenograft tumors in Nude mice. Our study provides experimental evidence for the *in vitro*

and *in vivo* anti-prostate cancer activities of THA, and suggest that further studies are warranted for the development of this compound as a new anticancer drug.

2. Materials and methods

2.1 Cells and reagents

Prostate cancer cell lines LNCaP, PC-3 and DU145, and the human normal prostate epithelial RWPE-1 cells were obtained from the American Type Culture Collection (ATCC, Rockville, MD, USA). RPMI-1640, MEM, DMEM and K-SFM culture medium, penicillin–streptomycin, L-glutamine and fetal bovine serum (FBS) were obtained from Gibco (Grand Island, NY). Human prostate cancer PC-3 cells and LNCaP cells were cultured in RPMI-1640 medium. DU145 cells were cultured in MEM medium. RWPE-1 cells were cultured using K-SFM medium. RPMI-1640, MEM and DMEM media were supplemented with 10% FBS, while K-SFM medium was supplemented with 0.05 mg/mL bovine pituitary extract (BPE) and 5 ng/mL human recombinant epidermal growth factor (EGF). The culture medium is supplemented with penicillin (100 μg/mL) - streptomycin (100 μg/mL) and L-glutamine (300 μg/mL). Cultured cells were grown at 37 ℃ in a humidified atmosphere of 5% CO_2 and were passaged twice a week.

2.2 MTT assay

PC-3, LNCaP, DU145 and RWPE-1 cells were seeded on 96-well plates at a density of 4 × 10^3 per well and incubated at 37 ℃ for 24 h. The cells were then treated with various concentrations of THA or paclitaxel (PTX) for 72 h. After treatment, 100 μL of MTT (3-(4,5-dimethylthiazol-2-yl)-2,5-diphenyltetrazolium bromide) solution (0.5 mg/mL in FBS free medium) was added to each of the wells of the plate and incubated at 37 ℃ for 4 h. After careful removal of the medium, 100 μL DMSO was added to each well. The absorbance was recorded on a microplate reader at 490 nm.

2.3 Cell migration assays

The cell migration ability was assessed using a scratch wound healing assay. In brief, cells were seeded at 5 × 10^5 cells per well in 12-well plates. When the cells were 95–100% confluent, media was removed and the cell surface was scratched using a sterile 200 mL pipette tip. Floating cells were removed by washing twice with PBS. Cultivation was subsequently continued for 24 h in 1% FBS medium. The cells were treated with THA or PTX.

2.4 Invasion assays

PC-3 cells (2 × 10^4 cells/well) were plated in serum-free RPMI-1640 in the top chamber with a membrane (24 well insert, pore size, 8 μm; Corning Inc., Corning, NY, USA) coated with Matrigel (1 mg/mL; BD Biosciences, San Jose, CA, USA). RPMI-1640 containing 15% FBS was used as a chemoattractant in the lower chamber. The cells were treated with PTX (2

nM) or THA at different concentrations separately for 24 hours. After the treatment, a cotton swab was used to remove the non-migrated cells in the upper chamber, and the membranes were stained with 2% crystal violet. The cells invaded through the Matrigel and migrated to the underside of the membrane were examined and counted under a light microscope.

2.5 Colony formation assay

Cells were seeded at 1×10^3 cells per well in 6-well plates and treated with PTX (2 nM) or THA at different concentrations separately for 24 hours and replaced with fresh media. Cells were grown for 5 days. In order to visualize the colonies, cells were fixed in methanol for 15 min and then stained with Giemsa for an additional 10 min.

2.6 Sphere-formation assay

Spheres were formed in keratinocyte serum-free medium in an ultra-low attachment plate. In brief, PC-3 cells were harvested from a monolayer culture and suspended in keratinocyte serum-free medium. The cells were seeded at a density of 1×10^3 cells/mL in each well and treated with PTX (2 nM) or THA at different concentrations for 24 hours, and then incubated at 37 ℃ for 14 days without disturbing the plates or replenishing the medium. At the end of the 14 day incubation, spheres were collected at the center of the well by slowly swirling the plates and examined using a microscope.

2.7 Flow cytometry detection of apoptosis and cell cycle

PC-3 cells in fresh complete medium were seeded in 6-well plates (6×10^4 cells/well) for 24 h. Then, the medium was removed and fresh medium containing different concentrations of THA was added and cultured again for 72 h. PTX was used as a positive control. After cultured, the cells were collected and washed twice with ice-cold PBS, binding buffer solution was added to the collected cell precipitation. Then 100 μL of cell suspension was reabsorbed into the new centrifuge tube, and cells were stained with 5 μL annexin-V-FITC and 10 μL propidium iodide (PI) using the Annexin V-FITC/PI Apoptosis Detection Kit (Yeasen Biotechnology Co, Ltd, Shanghai, China). After incubation at room temperature for 15 min (in dark place), 400 μL binding buffer was added to each well. Cells were then analyzed by flow cytometry using a CytoFLEX cytometer (Beckman Coulter, Inc., California, USA) and FlowJo program (Tree Star, Inc., Ashland, OR, USA). During the detection cycle, cells were fixed overnight with 70% ethanol, stained with PI, incubated for 30 minutes without light, and finally detected using a flow cytometer.

2.8 Hoechst-33342 staining

PC-3 cells were treated with THA at different concentrations in a 12-well plates (5×10^4 cells per well) for 72 h, followed by adding the Hoechst 33342 reagent (Sangon Biotech,

Shanghai, China) to each well, and then co-incubated for 30 min. Then cells were washed to remove extra dye and their images were obtained using an Olympus IX73 fluorescence microscope (Olympus Corporation, Japan).

2.9 Western blotting

The PC-3 cells in logarithmic growth stage were seeded at a density of 1×10^5 cells/well in a 6-well plate and incubated for 24 h. Afterwards, treat the cells with THA or PTX for 24 hours. Then, at the end of the experiment, cells from each treatment group were lysed using RIPA buffer (200 μL/well) to prepare cell lysate. The total protein content in each lysate was determined and and the proteins were separated by sodium dodecyl sulfate–polyacrylamide gel ectrophoresis and electrotransferred to a nitrocellulose membrane. After blocking nonspecific binding sites with 5% (w/v) skim milk powder, the membrane was incubated overnight at 4 ℃ with primary antibodies from Cell Signaling Technology (#9145 for p-STAT3, #9101 for p-p44/42, #15071 for Bcl-2, #2808 for survivin, and #9271 for p-AKT). β-actin (abs10041; Absin Bio, Shanghai, China) was used as a loading control. Subsequently, the membrane was washed three times with Tris-buffered saline for 1 h at room temperature, followed by incubation with a secondary antibody. Finally, the protein bands were detected using the Pierce™ ECL Western Blotting Substrate (Thermo Fisher Scientific).

2.10 STAT3, AKT and Erk1/2 siRNA transfection

PC-3 cells in logarithmic growth stage were seeded at a density of 1×10^5 cells/mL in 6-well plates and incubated for 24 h for cell adherence to the plates. Then, STAT3, AKT or Erk1/2 siRNA were transfected into the cells using Lipofectamine 3000 (Thermo Fisher Scientific) according to the manufacturer's instructions. The final concentration of siRNA was 100 nM. After 48 h, the cells were harvested for protein expression assays using the Western blotting or treated with THA for 24 h. After the treatment, cell viability was determined by the MTT assay.

2.11 Animal experiment

The animal experiment plan was reviewed and approved by the Experimental Animal Welfare and Ethics Committee of International Healthcare Innovation Institute (Jiangmen) (Approval Number: N2023023). The source and culture method of PC-3 cells were the same as those in **2.1**. Male BALB/c nude mice (4-6 weeks old) were purchased from Zhuhai Baishitong Biotechnology Co., Ltd. PC-3 cells were cultured *in vitro* to the logarithmic growth phase. After digestion and centrifugation, the cell suspension was adjusted to 9×10^7/mL. Afterward, PC-3 cells (6×10^6 cells) were mixed with Biozellen matrix® (Biozellen, USA) and then injected subcutaneously into the inguinal region of the mice. Approximately 5

to 7 days after successful establishment of the transplanted tumor animal model, when the subcutaneous tumor in nude mice reached a volume of approximately 70 mm^3, the animals were randomly assigned to four groups: the normal control group, the positive control group, the low-dose THA treatment group and the high-dose THA treatment group, with eight mice per group. THA was dissolved in DMSO and then diluted with the dilution vehicle, which consisted of propylene glycol, poly sorbate 80, benzyl alcohol, ethanol and water (40:0.5:1:10:48.5, v/v). Administration was performed via intraperitoneal injection. The control group received the dilution vehicle alone (200 μL), while the positive control group was administered PTX at a dose of 0.1 mg/kg. The THA treatment groups received doses of 2 mg/kg and 10 mg/kg, respectively. Treatments were administered continuously for 15 days. Tumor growth was measured every two days using calipers, and body weight changes were recorded throughout the study period. At the end of the treatment period, nude mice were euthanized by cervical dislocation, and tumors were excised, photographed, and measured for final tumor volume. All measurement data were subjected to statistical analysis.

2.12 Statistical analyses

All data of each treatment group from various experiments were presented as mean ± SEM. Statistical analysis of the data were carried out using a one-way ANOVA. A p-value < 0.05 was considered statistically significant.

3. Results

3.1 Treatment with THA reduces the viability of prostate cancer cells

The inhibitory effect of THA (Fig. 1A) on human prostate cancers was evaluated using the MTT assay in PC-3, DU145 and LNCaP cell lines. The results, as depicted in Fig. 1B, showed a dose-dependent decrease in cell viability after treatment with THA at concentrations of 0.1 μM, 0.5 μM, 1 μM, 2.5 μM and 5 μM for 72 hours. The IC_{50} values, calculated using the GraphPad software, were 2.4 μM, 2.4 μM, and 3.8 μM for PC-3, DU145 and LNCaP, respectively. By comparing the IC_{50} values, it was found that THA has a weaker inhibitory effect on the androgen-dependent LNCaP cells than that in the androgen-independent PC-3 and DU145 cells. This suggests that THA may have better therapeutic efficacy for advanced androgen-independent prostate cancer. Therefore, the PC-3 cell line was selected for subsequent experiments.

To investigate the potential toxicity of THA in normal cells, we determined the effect of this compound on normal prostate epithelial cell line RWPE-1. As shown in Fig. 1C, THA at the concentration range of 1-20 μM did not significantly reduce the survival rate of RWPE-1 cells, demonstrating no toxicity in normal cells and selectivity towards prostate cancer cells with this dose range. This result suggests that the concentrations selected in our experiment are within the safe window. Additionally, the effects of paclitaxel (PTX; served as positive control) were measured (Fig. 1D), and a dose dependent decrease in cell viability was found in PC-3 cells.

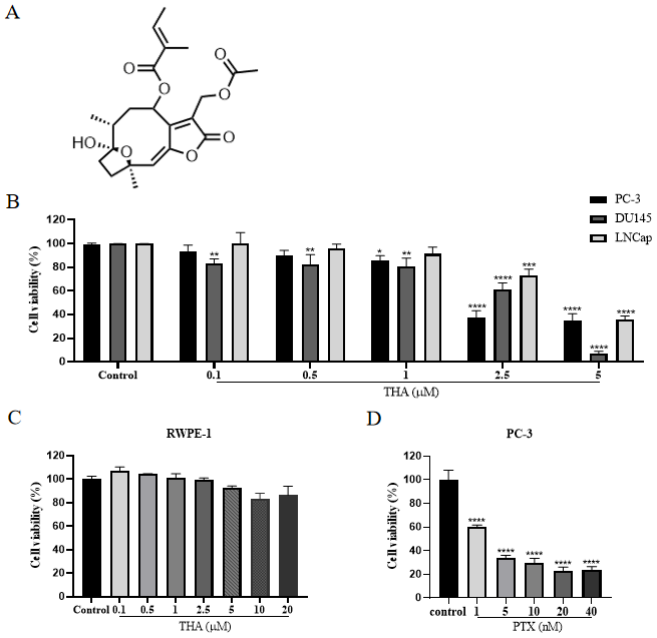

Fig. 1. Effects of THA on the viability of prostate cancer cells. (A) The chemical

structure of THA. (B) The cell viability (%) of PC-3 cells, DU145 cells and LNCap cells after treatment with THA (0.1 μM, 0.5 μM, 1 μM, 2.5 μM and 5 μM) for 72 hours. (C) The cell viability (%) of RWPE-1 cells with THA (0.1 μM, 0.5 μM, 1 μM, 2.5 μM, 5 μM , 10 μM and 20 μM) for 72 hours. (D) The cell viability (%) of PC-3 cells after treatment with PTX (1 nM, 5 nM, 10 nM , 20 nM, 40 nM) for 72 hours. Data are shown as mean ± standard deviation. *$p < 0.5$, **$p < 0.01$, ***$p < 0.001$, and ****$p < 0.0001$ compared with control.

3.2 THA inhibits the migration and invasion of PC-3 cells

The wound healing assay was used to record the area of blank regions at 0 h, 24 h, and 48 h to investigate the effect of THA on the migration ability of PC-3 cells. As compared to the control group, the THA treatment groups exhibited a significant inhibition of wound healing at 24 h and 48 h (Fig. 2A, 2C). At 24 h, the wound healing rates were 54.17±9.86% for the control group, and 32.2±1.40%, 28.08±3.87%, and 18.66±4.39% for the THA treatment groups at concentrations of 1 μM, 2.5 μM, and 5 μM, respectively ($p < 0.01$, $p < 0.001$, $p < 0.0001$). At 48 h, the control group had largely healed the wound area with a healing rate of 80.29±0.92%. The healing rates were 24.47±3.49% for THA (5 μM) and 53.79±7.62% for PTX (2 nM), both showing significant differences ($p < 0.0001$, $p < 0.001$). These results indicate that THA effectively inhibits the migration ability of PC-3 cells in a dose-dependent manner. The results of the transwell chamber assay (Fig. 2B, 2D) showed that the invasion rate for PTX (2 nM) was 53.8±11.9%. THA significantly reduced the number of PC-3 cells that passed through the chamber after 24 hours of treatment, with the lowest invasion rate observed at 5 μM 48.48±8.63%, shwing statistical significance ($p < 0.001$). These findings indicate that THA has a significant inhibitory effect on the invasive capability of PC-3 cells, suggesting its potential to reduce tumor cell metastasis and invasion.

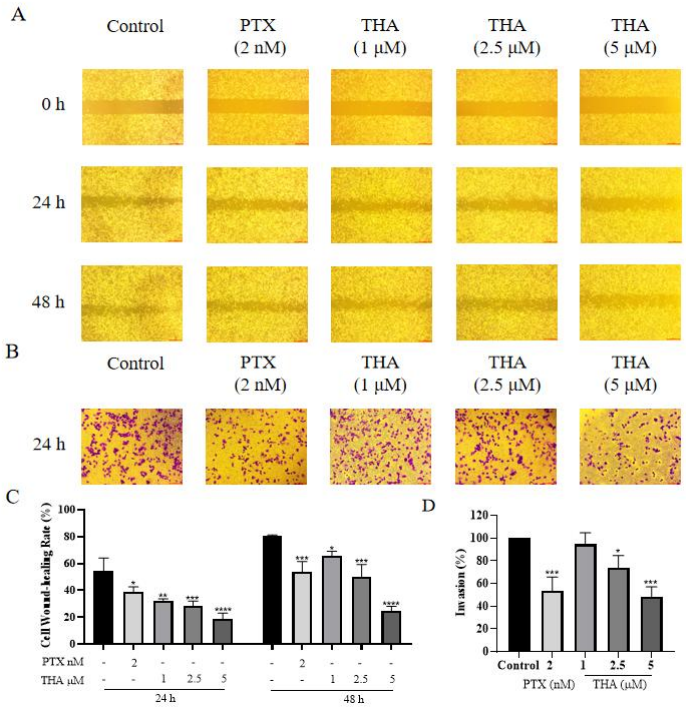

Fig. 2. Effects of THA on migration and invasion of PC-3 cells. (A)The effect on the migration ability of PC-3 cells after treatment with PTX (2 nM) or THA (1 μM, 2.5 μM and 5 μM) for 24 or 48 hours. (Scale bar, 500 μm). (B) The effect of on the invasion ability of PC-3 cells after treatment with PTX (2 nM) or THA (1 μM, 2.5 μM and 5 μM) for 24 hours. (Scale bar, 200 μm). (C) The cell wound-healing rate (%) of PC-3 cells after treatment with PTX (2 nM) or THA (1 μM, 2.5 μM and 5 μM) for 24 or 48 hours. (D) The invasion (%) of PC-3 cells after treatment with PTX (2 nM) or THA (1 μM, 2.5 μM, 5 μM) for 24 hours. Data are shown as mean ± standard deviation. *$p < 0.5$, **$p < 0.01$, ***$p < 0.001$, and ****$p < 0.0001$ compared with control.

3.3 THA Inhibits the formation of colony and tumor spheroid in PC-3 cells

The colony formation assay was employed to evaluate the effect of THA on the clonogenic ability of PC-3 cells. As shown in Fig. 3A and 3C, the colony formation rate of the PTX group was 31.0±7.01%. The colony formation rates of the THA treatment groups at concentrations of 1 μM, 2.5 μM, and 5 μM were 67.26±6.38%, 29.96±5.43%, and 2.91±1.02%, respectively, all of which were statistically significant as compared to the control ($p < 0.0001$). These findings demonstrate that THA significantly inhibited the colony forming ability of PC-3 cells. In additional experiments, the tumor sphere formation assay was conducted on PC-3 cells treated with THA. As shown in Fig. 3B and 3D, the number of PC-3 spheroids significantly decreased following treatment with THA, with the lowest

spheroid formation rate observed at 5 μM THA (13.64±6.43)% ($p < 0.0001$).

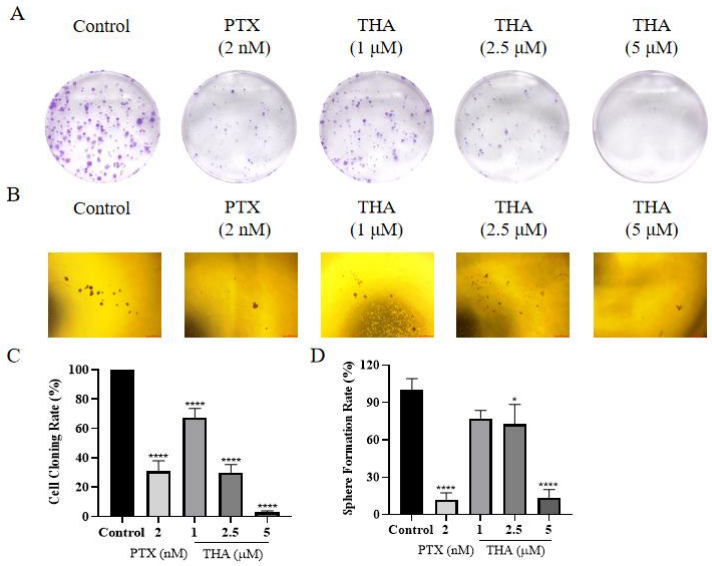

Fig. 3. Effects of THA on the formation of colony and spheroid in PC-3 cells. (A) The effect on the clonogenic ability of PC-3 cells after treatment with PTX (2 nM) or THA (1 μM, 2.5 μM and 5 μM) for 5 days. (B) The effect on the sphere formation ability of PC-3 cells after treatment with of PTX (2 nM) or THA (1 μM, 2.5 μM and 5 μM) for 14 days. (C) The cell cloning rate (%) of PC-3 cells after treatment with PTX (2 nM) or THA (1 μM, 2.5 μM and 5 μM) for 5 days. (Scale bar, 500 μm). (D) The sphere formation rate (%) of PC-3 cells after treatment with PTX (2 nM) or THA (1 μM, 2.5 μM and 5 μM) for 14 days. Data are shown as mean ± standard deviation. *$p < 0.5$ and ****$p < 0.0001$ compared with control.

3.4 Effects of THA on apoptosis in PC-3 cells and cell cycle in PC-3 cells

After treatment with THA, apoptosis in PC-3 cells increased significantly. At 5 μM, the early apoptosis rate was 44.70±12.88%, and the late apoptosis rate was 17.66±3.31%, which were significantly different from that in the control group ($p < 0.0001$) (Fig. 4A and 4D). The total apoptosis rate at 5 μM THA was 62.36±9.59%, compared to 33.0±4.80% for PTX (2 nM), with both showing significant differences ($p < 0.0001$, $p < 0.01$) (Fig. 4A and 4D). This finding suggests that THA may exert its anti-tumor activity by inducing apoptosis in PC-3 cells in a dose-dependent manner. On the other hand, using the Hoechst 33342 fluorescent dye, which serves as a live-cell nuclear marker, we observed changes in nuclear morphology following THA-induced apoptosis in PC-3 cells (Fig. 4B). After staining with Hoechst 33342 fluorescent dye, the nuclei of apoptotic cells displayed crescent-shaped or fragmented morphologies and emitted bright blue fluorescence.

Flow cytometry was employed to detect changes in the cell cycle distribution of PC-3

cells after treatment with THA to explore the effects of THA on the cell cycle of PC-3 cells. As shown in Fig. 4C, 4E and 4F, after 72 hours of treatment with THA at concentrations of 0, 1, 2.5, and 5 μM, the proportion of cells in the G0/G1 phase gradually decreased (from 74% to 47%), while the proportion of cells in the S phase gradually increased (from 14% to 38%), with no significant change observed in the G2/M phase. Analysis of the results showed that as the concentration of THA increased to 5 μM, the decrease in the G0/G1 phase and the increase in the S phase were statistically significant ($p < 0.001$, $p < 0.01$). PTX primarily affected the G2/M phase of the cell cycle, significantly increasing the proportion of cells in this phase ($p < 0.0001$), consistent with its mechanism of action, thereby ensuring the reliability of the experiment. The experiment demonstrated that THA primarily affected the mitotic phase (G2/M phase) of PC-3 cells, causing cell cycle arrest at the S phase, preventing progression to the G2/M phase, leading to an increase in the S phase and a decrease in the G0/G1 phase. This suggests that THA induces cell cycle arrest in PC-3 cells, which may result in increased apoptosis and decreased cell proliferation, thereby reducing the migration and invasion capabilities of the cells. This is because sufficient energy and metabolic resources are required for cell migration and invasion, and cell cycle arrest may lead to a reduction in these resources.

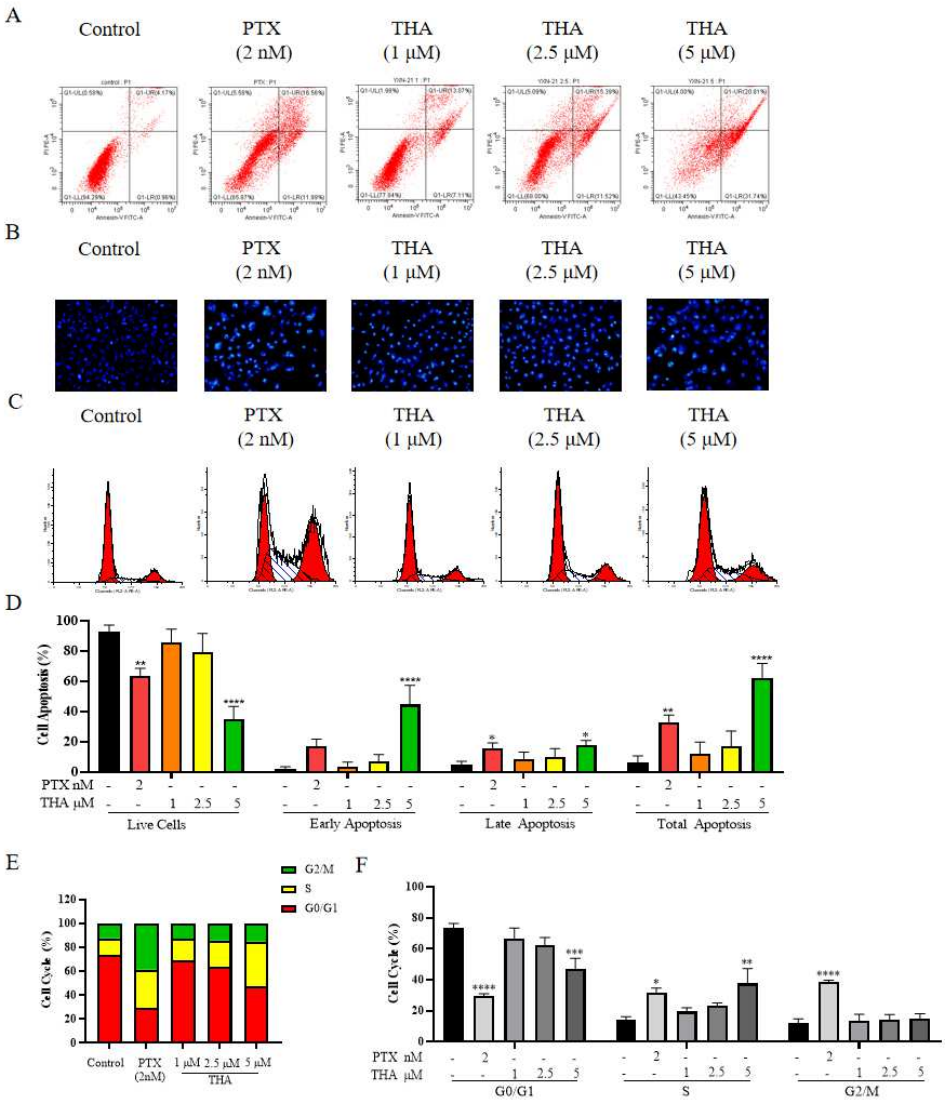

Fig. 4. Effects of THA on apoptosis in PC-3 cells. (A) THA induced apoptosis in PC-3 cells as assessed by Annexin-V FITC/PI assay, the result is from one experiment representative of three similar experiments. (B) Cells were stained with Hoechst 33342 and observed under a fluorescence microscope. (C) The effect on the apoptosis ability of PC-3 cells after treatment with PTX (2 nM) or THA (1 μM, 2.5 μM and 5 μM) for 72 h , (D) The percentage of viable cells, early apoptotic cells, late apoptotic cells and total apoptotic cells in untreated, PTX-treated and THA-treated PC-3 cells. (E) The cell cycle of PC-3 cells after treatment with PTX (2 nM) or THA (1 μM, 2.5 μM and 5 μM) for 72 h. (F) Cells were stained with PI was analyzed by flow cytometry. G0/G1, S and G2/M indicate the respective cell cycle phase. Data are shown as mean ± standard deviation. *$p < 0.5$, **$p < 0.01$, ***$p < 0.001$, and ****$p < 0.0001$ compared with control.

3.5 Effects of THA on STAT3, MMP9, survivin, AKT, Bcl-2, Bax, Erk1/2, cyclin E1 and CDK2

The expression levels of p-STAT3/STAT3 were detected by Western blot, revealing that THA significantly decreased the protein level of p-STAT3 (Fig. 5A). The levels of MMP9 (Fig. 5B) and survivin (Fig. 5C) which are downstream proteins of STAT3 were examined, and THA significantly inhibited the expression of these proteins. Additionally, the levels of p-AKT (Fig. 5D) and its downstream apoptotic protein targets Bcl-2 (Fig. 5E) and Bax (Fig. 5F) were assessed. As the concentration of THA increased, the ratio of Bcl-2 to Bax significantly decreased, potentially working in conjunction with survivin to increase the likelihood of apoptosis. THA showed inhibitory effects on p-Erk1/2 (Fig. 5G), cyclin E1 (Fig. 5H), and CDK2 (Fig. 5I) in PC-3 cells. The inhibition of Erk1/2 phosphorylation is involved in the THA-induced S-phase accumulation and apoptosis in PC-3 cells, consistent with previous experimental results (Fig. 5J). To further investigate the roles of STAT3, AKT, and Erk1/2 in the mechanism by which THA affects PC-3 cells, STAT3 siRNA (Fig. 6A), AKT siRNA (Fig. 6B), and Erk1/2 (Fig. 6C) siRNA were used for interference. The results showed that transfection with siRNA without drug treatment led to reduced cell viability. The viability of scramble siRNA-transfected cells treated with 5 μM THA was 54%, while the cell viability of STAT3 siRNA-transfected cells at the same concentration of THA was 72% (Fig. 6H). This demonstrates that the inhibitory effect of THA on cell viability was significantly attenuated ($p < 0.01$) by transfection with STAT3 siRNA (Fig. 6D). This result suggests that STAT3 plays a crucial role in mediating the inhibitory effect of THA on PC-3 cells. Moreover, cells transfected with AKT siRNA (Fig. 6I) and Erk1/2 siRNA (Fig. 6J) showed higher viability when treated with 5 μM THA compared to the scramble siRNA-transfected cells treated with same concentration of THA. This inhibitory effect of THA on cell viability was significantly weakened when the AKT ($p < 0.05$) and Erk1/2 ($p < 0.05$) genes were silenced (Fig. 6E and 6F). This result suggests that AKT and Erk1/2 play important roles in regulating the effects of THA on PC-3 cells .

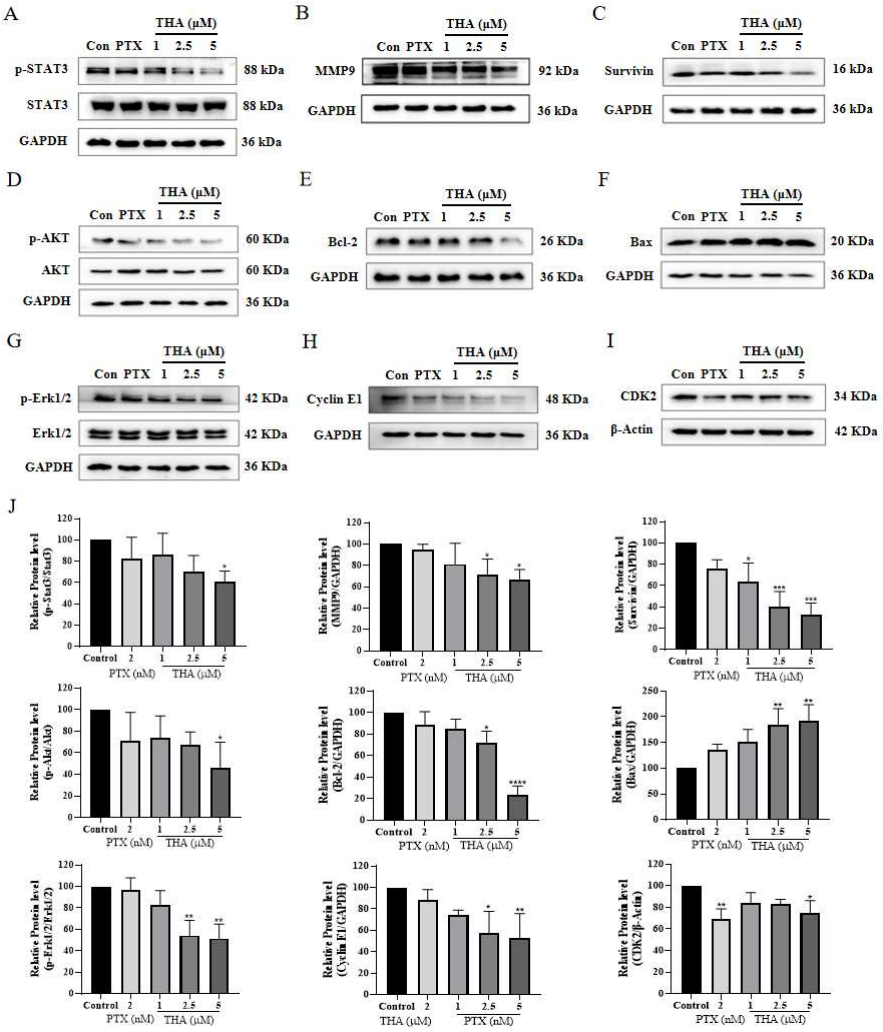

Fig. 5. Effects of THA on STAT3, MMP9, survivin, AKT, Bcl-2, Bax, Erk1/2, cyclin E1 and CDK2. Western blot results of STAT3 (A), MMP9 (B), survivin (C), AKT (D), Bcl-2 (E), Bax (F), Erk1/2 (G), cyclin E1 (H) and CDK2 (I) after treatment with PTX (2 nM) or THA (1 μM, 2.5 μM and 5 μM) for 72 h. (J)The relative protein level of STAT3, MMP9, survivin, AKT, Bcl-2, Bax, Erk1/2, cyclin E1 and CDK2 after treatment with PTX (2 nM) or THA (1 μM, 2.5 μM and 5 μM) for 72 h. Data are shown as mean ± standard deviation. *$p < 0.5$, **$p < 0.01$ and ****$p < 0.0001$ compared with control.

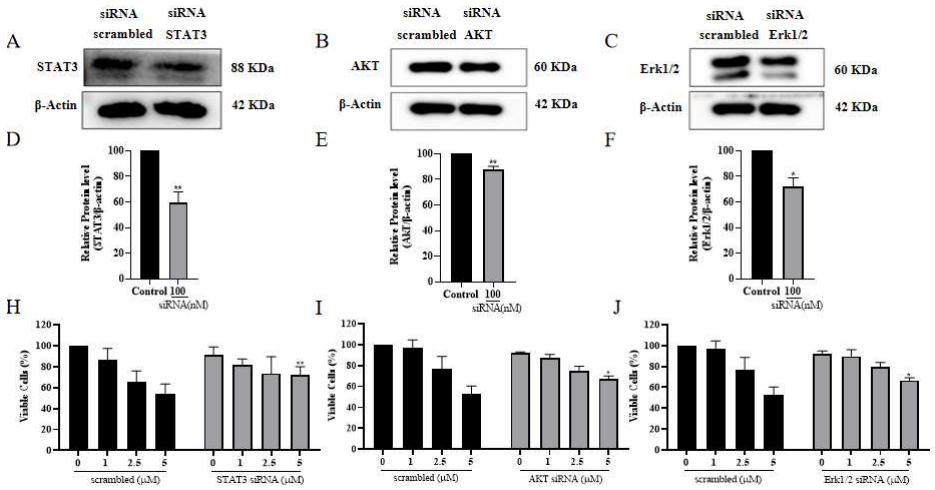

Fig. 6. Effects of THA on STAT3, AKT, Erk1/2. Western blot results of STAT3 (A), AKT (B) and Erk1/2 (C) after treatment with siRNA on PC-3 Cells, The relative protein level of STAT3 (D), AKT (E) and Erk1/2 (F) after treatment with siRNA on PC-3 cells, The viable cells of STAT3 (H), AKT (I) and Erk1/2 (J) after treatment with siRNA on PC-3 Cells. Data are shown as mean ± standard deviation. *$p < 0.5$ and **$p < 0.01$ compared with control.

3.6 THA Decreases the Growth of PC-3 Xenograft Tumors

A mouse PC-3 xenograft tumor model was established in nude mice to evaluate the antitumor activity of THA *in vivo*. A representative figure is shown in Fig. 7A. It can be observed with the naked eye that the tumor volume of the administration group is smaller than that of the control group. After 15 days of THA administration, the average volume of transplanted tumors in the control group was 1556 mm^3, that in the PTX group was 637.0 mm^3 ($p < 0.05$), and the tumor sizes in the low-dose and high-dose THA groups were 603.9 mm^3 ($p < 0.05$), and 454.5 mm^3 ($p < 0.01$), respectively. The results proved that the THA compound had a significant inhibitory effect on the growth of PC-3 xenograft tumors (Fig. 7C). As shown in Fig. 7B, there was no significant weight loss in the treated groups compared to the control group. THA had a significant inhibitory effect on the growth of xenograft tumors after 15 days of treatment, and the differences between the the control group and the high or low dose treated groups were statistically significant ($p < 0.01$). Hematoxylin-eosin (H & E) staining of the tumor sections was carried out to observe the morphology of the tumors from each group. Sections of the tumors from the control group showed dense tumor cells with tight junctions between cells. In treatment groups, the intercellular spaces were significantly loose. Nuclear condensation and necrosis in some areas could be observed indicating apoptosis occurred in the tumor tissues (Fig. 7D).

The levels of p-STAT3, p-AKT, p-Erk1/2, CDK2, cyclin E1, MMP9, Bcl-2/Bax and survivin in tumor samples from each group were determined by the Western blot analysis (Fig. 8A). Significant differences were observed between the control group and the low dose THA (2 mg/kg) treated group for the levels of MMP9 ($p < 0.05$), Bax ($p < 0.01$), Bcl-2 ($p < 0.05$), cyclin E1 ($p < 0.01$), CDK2 ($p < 0.05$), p-Erk1/2 ($p < 0.001$), p-AKT ($p < 0.01$). Significant differences were also observed between the control group and the high dose THA (10 mg/kg) treated group for the levels of MMP9 ($p < 0.0001$), Bax ($p < 0.001$), Bcl-2 ($p < 0.01$), cyclin E1 ($p < 0.001$), CDK2 ($p < 0.001$), p-STAT3 ($p < 0.01$), p-Erk1/2 ($p < 0.001$), p-AKT ($p < 0.0001$) (Fig. 8B-J).

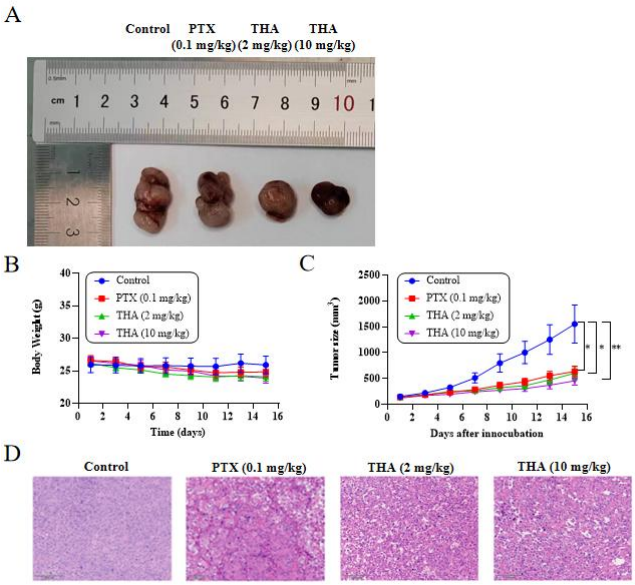

Fig. 7. Inhibitory effect of THA on PC-3 xenograft tumors. (A) Representative image of tumor sized under 0.1 mg/kg PTX, 2 mg/kg THA and 10 mg/kg THA treatments for 15 days. (B) The body weight of mouse for 15 days. (C) The Tumor size of mouse for 15 days. (D) H & E staining in xenograft tumors. (Scale bar, 200 μm). Data are shown as mean ± standard deviation. *$p < 0.5$ and **$p < 0.01$ compared with control.

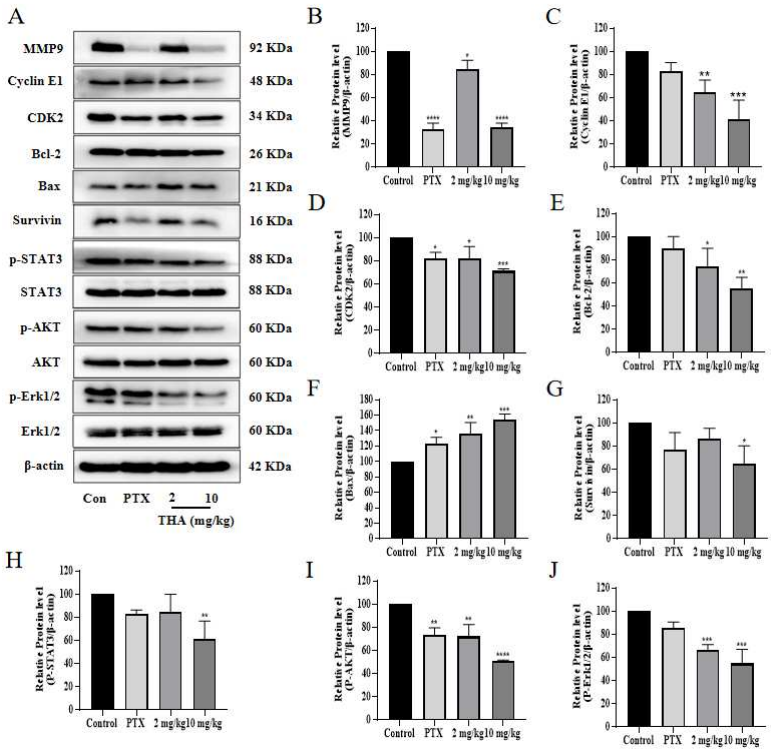

Fig. 8. Effects of THA on MMP9, cyclin E1, CDK2, Bcl-2, Bax, survivin, STAT3, AKT and Erk1/2, in PC-3 xenograft tumor model. (A) Western blot results of MMP9, cyclin E1, CDK2, Bcl-2, Bax, survivin, STAT3, AkT and Erk1/2. The relative protein level of MMP9 (B), cyclin E1 (C), CDK2 (D), Bcl-2 (E), Bax (F), survivin (G), STAT3 (H), AKT (I) and Erk1/2 (J). Data are shown as mean ± standard deviation. *$p < 0.5$, **$p < 0.01$, ***$p < 0.001$, and ****$p < 0.0001$ compared with control.

4. Discussion

In our effort to develop novel natural anti-prostate cancer agents, we isolated a series of natural compounds from *C. cinereum*. In initial screening experiments, our laboratory found that sesquiterpenoid compounds isolated from *C. cinereum* have anti-prostate cancer activities, and the hirsutinolide-type sesquiterpenoid (THA) showed the most potent inhibitory effect on prostate cancer cells (Ang et al. 2023). In the present study, we further investigated the anti-prostate cancer activities and mechanisms of actions for THA. We demonstrated for the first time that THA had strong *in vitro* and *in vivo* inhibitory effect on the growth of human prostate cancer cells. This compound also strongly inhibited prostate cancer cell migration, invasion and the formation of colony and tumor sphere.

Previous studies have shown that sesquiterpenoid lactones exhibit anti-cancer activities in human cancer cells including glioma, pancreatic, prostate, lung and gynecological cancer cells (Ang et al. 2023; Yan et al. 2022; Laurella et al. 2022; Fattahian et al. 2022; Yu et al. 2022). However, the mechanisms by which THA inhibits the growth and induces apoptosis in cancer cells are still largely unknown. In our present study, it was observed that THA decreased the levels of p-STAT3, indicating an inhibition on STAT3 activation in PC-3 cells. STAT3 is a transcription factor that regulates the expression of various genes involved in the regulation of cell proliferation, survival, differentiation, and apoptosis in various types of cancer (Liu et al. 2020; Zhang 2024). Reults from our present study indicate that the effects of THA on growth inhibition and apoptosis induction in prostate cancer PC-3 cells were associated with the inhibition of STAT3 signaling pathway.

Moreover, MMP9 and survivin, downstream proteins of STAT3 signaling pathway (Jia et al. 2017; Liu et al. 2015), were significantly inhibited in PC-3 cells after treatment with THA in our experiment. MMP9 is an important protease that plays a critical role in tumor invasion and metastasis. Its main function is to degrade matrix proteins and promote the migration and invasion of tumor cells (Mondal et al. 2020; Owyong et al.2019). Cell migration is the initial process of tumor cell metastasis, and cell invasion is one of the results of cell migration. Tumor cells escape the primary lesion through cell migration, then invade surrounding tissues through cell invasion, and ultimately settle in new locations to form metastatic tumors. The inhibitory effect of THA on cell migration and invasion observed in the present study was associated with a strong inhibition of MMP9. Survivin is an important apoptosis inhibitor protein, and its overexpression is associated with the occurrence, development, and drug resistance of tumors (Kondapuram et al. 2023; Fang et al. 2024). The levels of survivin was significantly decreased in THA treated PC-3 cells, suggesting that the

effect of this compound on apoptosis may be mediated at least in part by the inhibition of survivin.

In the present study, we also found that treatment of PC-3 cells with THA strongly decreased the levels of p-AKT and p-Erk1/2. MAPK/ERK and PI3K/AKT are signaling pathways frequently involved in tumorigenesis and tumor cell growth (Cao et al. 2019; Zhang et al. 2023). In addition, we found that Bcl-2 levels were significantly decreasd and Bax levels were increased in PC-3 cells after treatment with THA. It has been known that Bcl-2 and Bax are downstream apoptotic targets of MAPK/ERK and PI3K/AKT signaling pathways (Boucher et al. 2000; Liu et al. 2020). Increase in the protein levels of Bax and decrease in the levels of Bcl-2 promote apoptosis in cancer cells (Qian et al. 2022; Warren et al.2019). Our present study suggest that these proteins paly important role in apoptosis in PC-3 cells after treatment with THA. On the other hand, our result showed that THA caused accumulation of PC-3 cells in S phase, and this effect was associated with a decrease in CDK2 level. It has been known that CDK2 is required for terminating the S phase and driving the cell cycle transition from S phase to G2 phase (Ding et al. 2020; Ma et al. 2020; Okuda et al. 2000). Our result indicates that THA inhibits CDK2 leading to the cells accumulated in the S phase. Our study also showed that the levels of cyclin E1 were decreased in the cells treated with THA. However, it is unclear whether cyclin E1 plays any role in THA-induced S phase accumulation and further studies are needed. Moreover, results of the siRNA knocking down experiments confirmed that STAT3, AKT and Erk pathways were involved in the inhibition of PC-3 cells from THA. The results of our present study provide important clues for further in-depth mechanistic studies to fully understand the mechanisms of actions for THA.

The *in vivo* experimental results showed that THA significantly inhibited the growth of PC-3 tumors. There was no body weight loss in the animals and no toxic effect was found in major organs. In line with the results of *in vitro* studies, the Western blot analysis of the tumors samples showed that THA decreased the levels of p-STAT3, p-AKT and p-Erk1/2. This result indicates that the *in vivo* effect of THA on PC-3 tumor growth was associated with inhibition of STAT3, AKT and Erk signaling pathways. The decreased levels of Bcl-2 and survivin in tumor samples from mice in the treatment groups indicate that THA may induce apoptosis via the downregulation of these apoptosis related genes. Both *in vitro* and *in vivo* studies showed that MMP9 and CDK2 were decreased after treatment with THA indicating the these proteins contribute to the effects of THA on cell migration, invasion and cell cycle progression.

5. Conclusion

In conclusion, THA strongly inhibited cell growth and induced apoptosis, as well as caused cell cycle arrest at the S phase in PC-3 cells. THA also strongly suppressed cell migration and invasion, and decreased spheroid and colony formation. Animal experiment showed that THA inhibited the growth of PC-3 xenograft tumor in nude mice. Studies on mechanisms of actions showed that the potent anti-prostate cancer effects of THA were associated with inhibition of STAT3, AKT, and Erk1/2. Based on these findings presented above, THA represents a good candidate for further development of anti-prostate cancer agent.

Acknowledgements

The Figures were created by Adobe Photoshop (PS).

Author Contributions

Wenfeng Wang: Writing – original draft, Validation, Methodology, Investigation, Formal analysis, Data curation. Man Xiao: Validation, Formal analysis, Data curation. Peng Hong: Writing – original draft, Validation, Methodology, Investigation. Danyu Huang: Formal analysis, Writing – review & editing. Liting Liu: Validation, Data curation. Xi Zheng: Writing – review & editing, Supervision, Project administration, Funding acquisition, Conceptualization. Song Ang: Methodology, Formal analysis, Data curation. Dongli Li: Writing – review & editing, Supervision, Project administration, Funding acquisition. All authors have read and agreed to the published version of the manuscript. All authors reviewed the manuscript.

Funding

This work was supported by the National Natural Science Foundation of China (No. 82304323), Department of Education of Guangdong Province (No. 2022ZDJS025), the Guangdong Basic and Applied Basic Research Foundation (No. 2023A1515012904).

Availability of data and material

The datasets used and analysed during the current study are available from the corresponding author on reasonable request.

6. Ceclarations

Ethical Approval

All animal study was approved by the Ethics Committee of Jiangmen Health International Innovation Research Institute (No. N2023023) and were conducted in accordance with the National Guidelines for Laboratory Animal Welfare (GB/T 35892-2018, China).

Conflict of Interest

The authors declare that they have no known competing financial interests or personal relationships that could have appeared to influence the work reported in this paper.

7. References

Siegel RL, Giaquinto AN, Jemal A (2024) Cancer statistics. CA A Cancer J. Clin 74(1):12-49. https://doi.org/10.3322/caac.21820

McDonald J, O'Brien J, Kostos L, Lawrentschuk N, Azad A.A, Murphy D, Chen K (2022) Systemic therapy in metastatic hormone-sensitive prostate cancer. Curr Opin Support Palliat Care 16(4), 234-239. https://doi.org/10.1097/SPC.000000000000062

Desai K, McManus JM, Sharifi N (2021) Hormonal Therapy for Prostate Cancer. Endocr Rev 42(3):354-373. https://doi.org/10.1210/endrev/bnab002

Gulley J, Figg WD, Dahut WL (2003) Treatment options for androgen-independent prostate cancer. Clin Adv Hematol Oncol Jan 1(1):49-57.

Aparicio AM, Harzstark AL, Corn PG, Wen S, Araujo JC, Tu SM, Pagliaro LC, Kim J, Millikan RE, Ryan C, Tannir NM, Zurita AJ, Mathew P, Arap W, Troncoso P, Thall PF, Logothetis CJ (2013) Platinum-based chemotherapy for variant castrat e-resistant prostate cancer. Clin Cancer Res 19(13):3621-30. https://doi.org/10.1158/1078-0432/CCR-12-3791

Huebner NA, Shariat SF, Resch I, Gust K, Kramer G (2020) The role of taxane-based chemotherapy in the treatment of prostate cancer. Curr Opin Urol. 30(4):527-533. https://doi.org/10.1097/MOU.0000000000000784

Trang NM, Vinh LB, Phong NV, Yang SY. Traditional Uses (2024) Phytochemistry, and Pharmacological Activities of Vernonia cinerea (L.) Less. An Updated Review. Nutrients 16(9):1396. https://doi.org/10.3390/nu16091396

Sulaiman CT, Ramesh PR, Mahesh K, Anandan EM, Praveen M, Balachandran I (2022) Metabolite profiling of *Cyanthillium cinereum* (L.) H. Rob. and its herbal formulation by tandem mass spectroscopic analysis. Nat Prod Res 36(14):3726-3730. https://doi.org/10.1080/14786419.2020.1869972

Chadwick M, Trewin H, Gawthrop F, Wagstaff C (2013) Sesquiterpenoids lactones: be nefits to plants and people. Int J Mol Sci 14(6):12780-805. https://doi.org/10.3390/ijms140612780

Iwalewa EO, Iwalewa OJ, Adeboye JO (2003) Analgesic, antipyretic, anti-inflammatory effects of methanol, chloroform and ether extracts of *Vernonia cinerea* less leaf. J Ethnopharmacol 86(2-3):229-234. https://doi.org/10.1016/s0378-8741(03)00081-3

Neamsuvan O, Tuwaemaengae T, Bensulong F, Asae A, Mosamae K (2012) A survey of folk remedies for gastrointestinal tract diseases from Thailand's three southern border

provinces. J Ethnopharmacol 144(1):11-21. https://doi.org/10.1016/j.jep.2012.07.043

Lin KW (2005) Ethnobotanical study of medicinal plants used by the Jah Hut peoples in Malaysia. Indian J Med Sci 59(4):156-161.

Ang S, Liu C, Hong P, Yang L, Hu G, Zheng X, Jin J, Wu R, Wong WL, Zhang K, Gan L, Li D (2023) Hirsutinolide-type sesquiterpenoids with anti-prostate cancer activity from *Cyanthillium cinereum*. Phytochemistry 216:113887. https://doi.org/10.1016/j.phytochem. 2023.113887

Yan QL, Wang XY, Bai M, Zhang X, Song SJ, Yao GD (2022) Sesquiterpene lactones from *Elephantopus scaber* exhibit cytotoxic effects on glioma cells by targeting GSTP1. Bioorg Chem 129:106183. https://doi.org/10.1016/j.bioorg.2022.106183

Laurella LC, Mirakian NT, Garcia MN, Grasso DH, Sülsen VP, Papademetrio DL (2022) Sesquiterpene Lactones as Promising Candidates for Cancer Therapy: Focus on Pancreatic Cancer. Molecules 27(11):3492. https://doi.org/10.3390/molecules27113492

Fattahian M, Ghanadian M, Zolfaghari B, Aghaei M, Zulfiqar F, Khan IA, Ali Z (20 22) Phytochemical analysis of *Artemisia kopetdaghensis*: Sesquiterpene lactones wi th proapoptotic activity against prostate cancer cells. Phytochemistry 203:113411. https://doi.org/10.1016/j.phytochem.2022.113411

Yu PP, Yu F, Li WZ, Wang SM, Wang C, Dong M, Ni ZY, Li Y, Kiyota H (2021) Millifolide A, a dimeric ether of degraded sesquiterpene lactones, inhibited the proliferation of human lung cancer cell line A549. Nat Prod Res 36(11):2875-2877. https://doi.org/10.1080/14786419.2021.1922906

Liu Y, Liao S, Bennett S, Tang H, Song D, Wood D, Zhan X, Xu J (2020) STAT3 and its targeting inhibitors in osteosarcoma. Cell Prolif. 54(2):e12974. https://doi.org/ 10.1111/cpr.12974

Fang XL, Cao XP, Xiao J, Hu Y, Chen M, Raza HK, Wang HY, He X, Gu JF, Zhang KJ (2024) Overview of role of survivin in cancer: expression, regulation, functions, and its potential as a therapeutic target. J Drug Target 32(3): 223-240. https://doi.org/10.1080/ 1061186X.2024.2309563

Jia ZH, Jia Y, Guo FJ, Chen J, Zhang XW, Cui MH (2017) Phosphorylation of STAT3 at Tyr705 regulates MMP-9 production in epithelial ovarian cancer. PLoS One 31;12(8). https://doi.org/10.1371/journal.pone.0183622

Liu F, Zhang T, Zou S, Jiang B, Hua D (2015) B7-H3 promotes cell migration and invasion through the Jak2/Stat3/MMP9 signaling pathway in colorectal cancer. Mol Med Rep 12(4):5455-5460. https://doi.org/10.3892/mmr.2015.4050

Mondal S, Adhikari N, Banerjee S, Amin SA, Jha T (2020) Matrix metalloproteinase-9 (MMP-9) and its inhibitors in cancer: A minireview. Eur J Med Chem 194:112260. https://doi.org/10.1016/j.ejmech.2020.112260

Owyong M, Chou J, van den Bijgaart RJ, Kong N, Efe G, Maynard C, Talmi-Frank D, Solomonov I, Koopman C, Hadler-Olsen E, Headley M, Lin C, Wang CY, Sagi I, Werb Z, Plaks V (2019) MMP9 modulates the metastatic cascade and immune landscape for breast cancer anti-metastatic therapy. Life Sci Alliance. 2019:2(6): e201800226. https://doi.org/10.26508/lsa.201800226

Kondapuram SK, Ramachandran HK, Arya H, Coumar MS (2023) Targeting survivin for cancer therapy: Strategies, small molecule inhibitors and vaccine based therapeutics in development. Life Sci 335:122260. https://doi.org/10.1016/j.lfs.2023.122260

Fang XL, Cao XP, Xiao J, Hu Y, Chen M, Raza HK, Wang HY, He X, Gu JF, Zhan g KJ (2024) Overview of role of survivin in cancer: expression, regulation, functi ons, and its potential as a therapeutic target. J Drug Target 32(3):223-240. https:// doi.org/10.1080/1061186X.2024.2309563

Cao Z, Liao Q, Su M, Huang K, Jin J, Cao D (2019) AKT and ERK dual inhibitors: The way forward? Cancer Lett 459:30-40. https://doi.org/10.1016/j.canlet.2019.05.025

Zhang X, Chen J, Xi B, Liu Y, Wang S, Gu L, Zhao H, ao L, Hua Y, Wang Y, Chen M (2023) Agrimoniin is a dual inhibitor of AKT and ERK pathways that inhibit pancreatic cancer cell proliferation. Phytother Res 37(9):4076-4091. https://doi.org/10.1002/ptr.7867

Boucher MJ, Morisset J, Vachon PH, Reed JC, Lainé J, Rivard N (2000) MEK/ERK signaling pathway regulates the expression of Bcl-2, Bcl-X(L), and Mcl-1 and promotes survival of human pancreatic cancer cells. J Cell Biochem 79(3): 355-69.

Liu R, Chen Y, Liu G, Li C, Song Y, Cao Z, Li W, Hu J, Lu C, Liu Y (2020) PI3K/AKT pathway as a key link modulates the multidrug resistance of cancers. Cell Death Dis 11(9):797. https://doi.org/10.1038/s41419-020-02998-6

Qian S, Wei Z, Yang W, Huang J, Yang Y, Wang J (2022) The role of BCL-2 famil y proteins in regulating apoptosis and cancer therapy. Front Oncol 12:985363. htt ps://doi.org/10.3389/fonc.2022.985363

Warren CFA, Wong-Brown MW, Bowden NA (2019) BCL-2 family isoforms in apoptosis and cancer. Cell Death Dis 10(3):177. https://doi.org/10.1038/s41419-019-1407-6

Ding L, Cao J, Lin W, Chen H, Xiong X, Ao H, Yu M, Lin J, Cui Q (2020). The roles of cyclin-dependent kinases in cell-cycle progression and therapeutic strategies in human breast cancer. Int J Mol Sci 21(6):1960. https://doi.org/10.3390/ijms21061960

Ma JH, Qin L, Li X (2020) Role of STAT3 signaling pathway in breast cancer. Cell Commun Signal 18(1):33. https://doi.org/10.1186/s12964-020-0527-z

Okuda M, Horn HF, Tarapore P, Tokuyama Y, Smulian AG, Chan PK, Knudsen ES, Hofmann IA, Snyder JD, Bove KE, Fukasawa K (2000). Nucleophosmin/B23 is a target of CDK2/cyclin E in centrosome duplication. Cell. 103(1):127-140.https://doi.org/10.1016/s0092-8674(00)00093-3